HOKKAIDO UNIVERSITY

1

2

Environmental influences over the last 16 ka on compound-specific δ^{13}C variations

of leaf wax *n*-alkanes in the Hani peat deposit from northeast China

5

Shinya Yamamoto [a], *, Kimitaka Kawamura [a], Osamu Seki [a], Philip A. Meyers [a,b],

Yanhong Zheng [c], Weijian Zhou [d]

8

[a] Institute of Low Temperature Sciences, Hokkaido University, N19W8, Kita-ku,

Sapporo 060-0819, Japan

[b] Department of Geological Sciences, The University of Michigan, Ann Arbor,

Michigan, 48109-1005, U.S.A.

[c] State Key Laboratory of Continental Dynamics, Department of Geology,

Northwest University, Xi'an, 710069, China

[d] State Key Laboratory of Loess and Quaternary Geology, Institute of Earth

Environment, Chinese Academy of Sciences, Xi'an 710075, China

17

* Corresponding author. Tel: +81-11-706-5503; Fax: +81-11-706-7142

E-mail address: s.yamamoto@pop.lowtem.hokudai.ac.jp (S. Yamamoto)

Institute of Low Temperature Sciences, Hokkaido University, N19W8, Kita-ku, Sapporo

060-0819, Japan

22

22   **Abstract**

23   Compound-specific carbon isotope ratios ($\delta^{13}C$) of leaf wax n-alkanes (C_{21}-C_{33} odd

24   carbon numbered n-alkanes) were measured in the Hani peat sequence from northeast

25   China. These data were compared with lipid biomarker compositions to assess changes

26   in local vegetation and paleoclimate for the last 16 ka. The $\delta^{13}C$ values of n-alkanes

27   range between –36.6 to –30.7‰, showing that the compounds originate from C_3 plants.

28   Much larger variations (~5.4‰) in the n-alkane $\delta^{13}C$ values than those of atmospheric

29   CO_2 during the last 16 ka (< 0.5‰) indicate that the isotopic values were affected by

30   environmental factors in addition to the postglacial $\delta^{13}C$ variations in the atmospheric

31   reservoir. The stratigraphic records of $\delta^{13}C$ reveal decoupled fluctuations among the

32   individual n-alkanes, particularly between 15.5 to 11.4 ka. Synchronous excursions in

33   the $\delta^{13}C$ offsets among individual n-alkanes ($\Delta\delta^{13}C$) and lipid biomarker paleoplant

34   proxies (Paq, and C_{23}/C_{31} and C_{27}/C_{31}) from 14.9 to 13.2 ka and 12.7 to 11.6 ka suggest

35   that vegetational changes are the most likely causes for the decoupled $\delta^{13}C$ variations.

36   Parallel fluctuations of the $\delta^{13}C$ values of terrestrial higher plant-derived C_{29} and C_{31}

37   n-alkanes and the n-alkane average chain-length (ACL) from 11 to 6 ka indicate that the

38    $\delta^{13}C$ variations responded to net evaporation changes. Negative shifts in the n-alkane

39    $\delta^{13}C$ values coinciding with the ACL decreases at 10.5-9.3 ka and 8.1 ka indicate the

40   short-term onset and fluctuations of the summer monsoon strength in eastern China

41   during the early Holocene.

42

43   Keywords: peat; stable carbon isotopes; n-alkane; leaf wax; Holocene; Asian monsoon

44

45   **1. Introduction**

46   A peat deposit, which is an accumulation of partially decomposed and

47   thermally immature organic matter that is mainly composed of autochthonous vascular

48   plant debris, holds valuable information about continental paleoenvironmental histories

49   (Blackford, 2000). The kind and abundance of bog vegetation that contributes to a peat

50   sequence can be significantly influenced by local factors such as bog surface moisture

51   conditions, ground water level, influx of nutrient-rich groundwater, and lateral variety in

52   plant communities, while regional climate changes can affect bog vegetation and its

53   preservation in the peat sequence through the hydrology. Plant fossil records in the peat

54   can therefore serve as a proxy for past climate changes (Barber, 1985). Indeed, various

55   studies have reconstructed paleoenvironmental histories of peat bogs using pollen, plant

56   macrofossils and the stable carbon and oxygen isotopic compositions of plant cellulose

57   (Pendall et al., 2001; Hong et al., 2001; Xu et al., 2006; Schröder et al., 2007), as well

58   as other proxies like humification indices (Blackford and Chambers, 1993; Baker et al.,

59   1999; Wang et al., 2004) and testate amoebae (Charman, 2001).

60   Molecular compositions of lipid biomarkers derived from peat-forming plants

61   have also been shown to be important proxies to reconstruct past changes in bog

62   environments (Ficken et al., 1998; Nott et al., 2000; Pancost et al., 2002; Xie et al.,

63   2004; Zhou et al., 2005; Zheng et al., 2007; López-Díaz et al., 2010). Records of peat

64   n-alkanes are particularly robust because of their low susceptibility to microbial

65   degradation relative to other types of lipid compound classes (Meyers, 2003; Zheng et

66   al., 2007; Zhou et al., 2010), and their preferential production in the plant leaves rather

67   than the roots (Pancost et al., 2002) make their stratiform depositional records

68   preferable for paleoenvironmental archives, especially in a bog where plant

69   macrofossils are sometimes poorly preserved.

70   Several studies have also employed compound-specific carbon isotopic

71   analyses of n-alkanes to obtain additional paleoenvironmental information (Ficken et al.,

72   1998; Xie et al., 2004). Because the individual leaf wax n-alkanes in a peat bog

73   originate from a mixture of various types of vegetation with specific n-alkane

74   distributions and carbon isotopic compositions (δ^{13}C) (e.g. Corrigan et al., 1973; Ficken

75   et al., 1998; Yudina and Savel'eva, 2008), a combination of n-alkane distributions and

3

76 their $\delta^{13}C$ values can make it possible to identify changes in the contributing plant

77 species. Furthermore, the $\delta^{13}C$ of terrestrial and peat-forming C_3 plants is partially

78 controlled by isotopic fractionations that reflect physiological responses to conditions in

79 their growing environment, such as humidity, temperature, and light level (Arens et al.,

80 2000; Hong et al., 2001). Thus, the leaf wax $\delta^{13}C$ values may also provide information

81 about the local paleoenvironment.

82   In the northeastern part of China, Holocene peat mires and lakes are widely

83 distributed, some of which have been intensively studied to reconstruct the Holocene

84 climate changes that were induced by variations in the Asian monsoon activity. For

85 example, paleoenvironmental proxies such as paleo-lake levels, pollen and

86 loess/paleosol records have revealed an increase in summer monsoon precipitation

87 during the last deglaciation and the early Holocene (An et al., 2000 and references

88 therein). Recently, the stable carbon and oxygen isotopic compositions of plant cellulose

89 (Hong et al., 2005, 2009a) and the molecular and hydrogen isotopic compositions of

90 lipid biomarkers (Seki et al., 2009; Zhou et al., 2010) have been examined in the Hani

91 peat deposit from northeastern China to reconstruct paleoclimatic history for the last 16

92 ka.

93   In this study, we present the $\delta^{13}C$ profiles of leaf wax n-alkanes in the Hani

94 peat sequence, and we use these profiles to reconstruct paleoenvironmental changes that

95 are recorded in the $\delta^{13}C$ of terrestrial higher plants. The combination of the $\delta^{13}C$ and

96 molecular distribution of n-alkanes allows us to estimate changes in source vegetation

97 and paleoclimatic history in northeastern China over the last 16 ka.

98

99 **2. Experimental**

100 **2.1. Setting and stratigraphy of the Hani peat deposit**

101   The Hani peat bog (42°13'N, 126°31'E) is located near Liangshui in Jilin

102 Province (Fig. 1) at an elevation of 900 m and is surrounded by the numerous volcano

4

103   cones and crater lakes that form the Long Gang volcanic field. The peat covers an area

104   of 16.8 km^2 in a percolation mire where the Hani River has its source, and the stable

105   swampy environment has allowed development of a peat layer more than 9 m thick

106   since the end of the Last Glacial Maximum.

107   A core of the 963 cm thick peat sequence was recovered from near the center of

108   the Hani bog. It is mainly composed of peat of various colors with occasional

109   intercalations of mud and sand layers. The basal 33 cm of the core is marked with a

110   dark gray mud layer, which is followed by a 204 cm-thick black-brown peat layer. The

111   interval between 726 and 126 cm below the bog surface consists mainly of dark-brown

112   peat. A mixed layer of light-brown peat with coarse sand and a layer of light-brown peat

113   with abundant plant debris are intercalated at 640-606 and 316-246 cm depth intervals,

114   respectively. The uppermost 126 cm interval near the surface is composed of 60

115   cm-thick brown peat and 40 cm-thick light-brown peat layers, in ascending order, which

116   is capped with 26 cm of undegraded grass fragments (Fig. 2).

117   We developed an age-depth model based on calibrated calendar ages that were

118   obtained from accelerator mass spectrometry (AMS) ^{14}C ages provided by Zhou et al.

119   (2010) using CALIB 4.3 software (Stuiver and Reimer, 1993; Stuiver et al., 1998; Fig.

120   2). The peat accumulation rate averages 62 cm/ka, and the basal age of the entire 960

121   cm core sequence is 15.5 ka.

122

123   **2.2. Lipid analyses**

124   The samples consist of 1 cm sediment slices taken every 10 cm in the core.

125   Lipids were ultrasonically extracted with CHCl$_3$ from ca. 1-2 g of freeze dried sample at

126   the State Key Laboratory of Loess and Quaternary Geology in Xi'an, China. The

127   extracts were concentrated on a rotary evaporator under vacuum and taken to dryness

128   with a N$_2$ stream (Seki et al., 2009; Zhou et al., 2010). Aliphatic hydrocarbons were

129   isolated using silica gel column chromatography (230-400 mesh; 1% H$_2$O deactivated)

130   by elution with 1.5 ml *n*-hexane at the Institute of Low Temperature Science, Hokkaido

131   University.

132   Analysis of aliphatic hydrocarbon fractions was performed using gas

133   chromatography (GC) and GC/mass spectrometry (MS). GC analysis was performed

134   using a Hewlett-Packard 6890 gas chromatograph equipped with an on-column injector,

135   CP-Sil 5 CB fused silica column (60 m × 0.32 mm i.d., 0.25 μm film thickness) and a

136   flame ionization detector (FID). Helium was used as carrier gas. The GC oven

137   temperature was programmed from 50 to 120°C at 30°C/min, from 120 to 310 °C at

138   6 °C/min, and then held isothermally for 15.5 min. GC/MS analysis was performed

139   using a Hewlett-Packard 5973 Mass Selective Detector coupled to a Hewlett-Packard

140   6890 gas chromatograph equipped with a HP-5MS fused silica column (30 m × 0.25

141   mm i.d., 0.25 μm film thickness). The temperature program was the same as for the GC

142   analysis. The compounds were identified on the basis of their mass spectra, GC

143   retention times, and comparison with literature mass spectra.

144

145   **2.3. Compound-specific stable carbon isotope analysis**

146   In order to improve the accuracy of the compound-specific stable carbon isotope

147   ratio (δ^{13}C) analyses, the *n*-alkane fractions were purified using the urea adduct

148   technique of Yamamoto and Kawamura (2010). Briefly, a saturated solution of urea in

149   methanol was added to the hydrocarbon fraction dissolved in *n*-hexane/acetone (2:1)

150   and gently stirred overnight using a mechanical stirrer to complete the adduction. After

151   adduction, the solvent was removed from the urea precipitate, which was rinsed with

152   fresh solvent (*n*-hexane/acetone, 2:1) three times to remove non-adducted materials.

153   The urea crystals were dried under a N_2 stream and the *n*-alkanes were recovered in

154   *n*-hexane after dissolution of the crystals in water.

155   ^{13}C/^{12}C ratios of the purified *n*-alkanes were determined using a HP 6890 GC

156   coupled to a Finnigan MAT Delta Plus isotope ratio mass spectrometer via a Finnigan

157   MAT combustion furnace maintained at a temperature of 850 °C. The GC was equipped

158   with HP-5MS fused silica column (30 m × 0.32 mm i.d., 0.25 μm film thickness). The

159   GC oven was programmed from 50 to 120 °C at 30 °C/min, from 120 to 310 °C at

160   5 °C/min, and then held isothermally for 22 min. One to 2 μl of sample solution were

161   injected into the GC via an on-column injector with an internal standard of known

162   isotopic composition (C_{20} n-alkanoic acid methyl ester; $\delta^{13}C$ = –26.21‰). The $\delta^{13}C$

163   values are expressed as per mil (‰) relative to the Vienna Pee Dee Belemnite (VPDB).

164   Most measurements were duplicated. Reported $\delta^{13}C$ data represent an averaged value of

165   the duplicate analyses. An external standard consisting of C_{16} to C_{30} n-alkanes of known

166   isotopic compositions was daily injected into the GC/IRMS system to check the data

167   quality and to ensure that the analytical error of the n-alkanes remained below ±0.5‰

168   during the analyses (Bendle et al., 2007).

169

170   **3. Results and Discussion**

171   **3.1. $\delta^{13}C$ values of leaf wax n-alkanes in the Hani peat core**

172   The Hani peat core samples contain C_{21} to C_{35} n-alkanes with a strong

173   odd-over-even carbon number predominance (CPI = 3.1 to 7.5) as major aliphatic

174   hydrocarbons (Fig. 2). Generally, submerged and floating macrophytes contain a large

175   proportion of n-alkanes that maximizes at C_{21}, C_{23}, or C_{25}, whereas vascular land plants

176   and emersed macrophytes contain C_{27}, C_{29} and C_{31} n-alkanes as constituents of their

177   epicuticular waxes (e.g. Eglinton and Hamilton, 1967; Corrigan et al., 1973; Cranwell,

178   1984; Rieley et al., 1991; Ficken et al., 2000). Distribution patterns of these n-alkanes

179   show significant variations throughout the core (Fig. 2), suggesting variable

180   contributions from both types of plants.

181   Fig. 3 presents the profiles of the stable carbon isotopic compositions ($\delta^{13}C$)

182   of C_{21} to C_{33} odd carbon number n-alkanes in the Hani peat core. The $\delta^{13}C$ values of leaf

183   wax n-alkanes in the peat samples range from –36.6 to –30.7‰ (Fig. 3), which is in the

184 range of the $\delta^{13}C$ values reported for leaf wax n-alkanes in various Far East C_3 plants

185 (Chikaraishi and Naraoka, 2003) and in surface soil samples from eastern China

186 dominated by C_3 broad leaved forests (Rao et al., 2009). Inasmuch as cellulose $\delta^{13}C$

187 values have revealed that the contemporary vegetation in the Hani peat bog is

188 dominated by C_3 plant species (Hong et al., 2005), the leaf waxes likely originate from

189 the C_3 vegetation that flourished in the Hani peat bog. The $\delta^{13}C$ values of the leaf wax

190 n-alkanes are, however, ca. 8‰ isotopically depleted in ^{13}C compared with those in the

191 plant cellulose (Hong et al., 2005). Such depletion in leaf wax n-alkanes relative to peat

192 cellulose reflects increased carbon isotopic fractionation between lipids and plant

193 tissues in the acetate-malonate biosynthetic pathway (Collister et al., 1994).

194 The $\delta^{13}C$ of C_3 plants is partially controlled by the isotopic fractionations that

195 are affected by various ecological and physiological factors and the species composition

196 of their source vegetation (Arens et al., 2000), in addition to the isotopic composition of

197 atmospheric CO_2. Much larger variations (~5.4‰) in leaf wax n-alkanes (Fig. 3) than

198 those of atmospheric CO_2 during the last 16 ka (~0.5‰; Leuenberger et al., 1992)

199 indicate that the $\delta^{13}C$ variations were mainly controlled by factors other than the

200 postglacial $\delta^{13}C$ variations in the atmospheric reservoir.

201

202 **3.2. Impact of vegetational changes on the $\delta^{13}C$ of leaf wax n-alkanes**

203 Our records of the compound-specific $\delta^{13}C$ values show decoupled

204 fluctuations among the individual n-alkanes (Fig. 3). In particular, the decoupling is

205 prominent in the 960 to 650 cm interval where the $\delta^{13}C$ values of the C_{25} and C_{27}

206 n-alkanes decrease to as low as –36.6‰ in contrast to the smaller fluctuations from

207 –34.8 to –30.7‰ in the $\delta^{13}C$ values of the other n-alkanes (C_{21}, C_{23}, C_{29}, C_{31} and C_{33})

208 (Fig. 3). In the lower half of this interval (960 to 739 cm), the $\delta^{13}C$ profiles of the C_{23}

209 and C_{25} n-alkanes exhibit a 2.0 to 2.5‰ negative shift, but equivalent shifts are not

210 observed in the other n-alkane records. In the upper half of the interval (739 to 650 cm),

8

211   although C_{21} to C_{29} n-alkane profiles show concurrent $\delta^{13}C$ negative shifts, the

212   magnitudes of the shifts are significantly different among the compounds: those for C_{25}

213   and C_{27} are ca. 3.8‰, whereas those for the other n-alkanes are only 1.5 to 2.0‰ (Fig.

214   3).

215   The leaf wax n-alkanes in a peat bog are commonly derived from an

216   assemblage of different plants, each with specific n-alkane distributions and $\delta^{13}C$ values

217   (Ficken et al., 1998). Hence, the decoupling in the $\delta^{13}C$ variations of n-alkanes with

218   different chain-lengths may indicate that the $\delta^{13}C$ values of individual n-alkanes reflect

219   changes in plant community compositions that contribute to the peat n-alkanes. In

220   support of this idea, pollen records from Lake Sihailongwan, northeast China, have

221   revealed a gradual transition from steppe and open taiga-like woodland communities

222   during the late glacial to the earliest Holocene toward the dense deciduous forests that

223   are similar to modern flora (Schettler et al., 2006; Stebich et al., 2009). Similarly, the

224   ecophysiological responses to environment stresses may have been different among the

225   assemblage of peat-forming plants, which would further emphasize the $\delta^{13}C$ offsets

226   among individual compounds.

227   In this study, we assessed the possible impact of changes in the plant

228   communities on the $\delta^{13}C$ variations by comparison with the Paq and the concentration

229   ratios of the C_{21} to C_{33} odd carbon number n-alkanes against the C_{31} n-alkane. The Paq

230   (Ficken et al., 2000) is a paleoplant proxy expressed by the following equation:

231   Paq = $(C_{23}+C_{25})/(C_{23}+C_{25}+C_{29}+C_{31})$

232   that can reveal the proportion of aquatic (submerged and floating) macrophytes to total

233   peat forming plant taxa and has already been shown to be informative in the Hani peat

234   deposit (Seki et al., 2009; Zhou et al., 2010). The n-alkane ratios, especially the C_{27}/C_{31}

235   and C_{23}/C_{31} ratios are also known as paleoplant proxies. The C_{27}/C_{31} concentration ratio,

236   which was originally described as C_{31}/C_{27} ratio in Schwark et al. (2002), is generally

237   considered to express the relative contribution of C_3 grasses whose leaf wax n-alkanes

238   are dominated by the C_{31} homologue. However, the dominant *n*-alkane chain-lengths in

239   contemporary vegetation at the Hani peatland (Table 1) and the surrounding mountains

240   (Schröder et al., 2007; Makohonienko et al., 2008) from the literature suggest that the

241   C_{31} *n*-alkane may also be supplied to the peat deposit by some mosses and trees (e.g.

242   *Juglans*, *Betula*, *Abies*, *Taxus*, *Tilia*, *Fraxinus* and *Larix*) besides C_3 grasses. In contrast,

243   the C_{23}/C_{31} concentration ratio can represent the contribution of *Sphagnum* species

244   (Pancost et al., 2002). It is based on the observation that *Sphagnum* yields preferentially

245   C_{23} and C_{25} *n*-alkanes compared to other homologues (Ficken et al., 1998; Nott et al.,

246   2000; Pancost et al., 2002; Table 1).

247   In Fig. 4, we compare the profiles of the P*aq* and the *n*-alkane biomarker

248   ratios with those of the $\delta^{13}C$ offsets between the C_{31} *n*-alkane and the C_{21}, C_{23}, C_{25}, C_{27},

249   C_{29} and C_{33} *n*-alkanes; hereafter expressed as $\Delta\delta^{13}C$ $(C_{31} - C_{21})$, $\Delta\delta^{13}C$ $(C_{31} - C_{23})$, $\Delta\delta^{13}C$

250     $(C_{31} - C_{25})$, $\Delta\delta^{13}C$ $(C_{31} - C_{27})$, $\Delta\delta^{13}C$ $(C_{31} - C_{29})$ and $\Delta\delta^{13}C$ $(C_{31} - C_{33})$, respectively. The

251     $\Delta\delta^{13}C$ records reveal significant positive excursions from 14.9 to 13.2 ka and 12.7 to

252   11.6 ka, although the magnitudes of the excursions of $\Delta\delta^{13}C$ $(C_{31} - C_{21})$, $\Delta\delta^{13}C$ $(C_{31} -$

253     $C_{29})$ and $\Delta\delta^{13}C$ $(C_{31} - C_{33})$ are much smaller than those of $\Delta\delta^{13}C$ $(C_{31} - C_{23})$, $\Delta\delta^{13}C$ $(C_{31}$

254     $- C_{25})$ and $\Delta\delta^{13}C$ $(C_{31} - C_{27})$ (Figs. 4a, b). The simultaneous changes in paleoplant

255   proxies with the excursions strongly suggest that vegetational changes are the most

256   likely causes for the decoupled variations among the *n*-alkane homologues. Changes in

257   the sedimentary environment may also have potentially affected the $\delta^{13}C$ values through

258   the enhancement of allochthonous plant input from the surrounding forests. However, a

259   lack of any clear relation between the $\delta^{13}C$ variations and the peat lithology suggests

260   that such an increase is unlikely.

261

262   *3.2.1. Vegetational change from 14.9 to 13.2 ka*

263   Parallel increases in the C_{23}/C_{31} ratios and the $\Delta\delta^{13}C$ $(C_{31} - C_{23})$, $\Delta\delta^{13}C$ $(C_{31} -$

264     $C_{25})$, $\Delta\delta^{13}C$ $(C_{31} - C_{27})$ and $\Delta\delta^{13}C$ $(C_{31} - C_{29})$ values from 14.9 to 13.2 ka (Figs. 4a-4c)

265   indicate that a relative increase in the contribution of *Sphagnum* species to the peat

266   *n*-alkanes is the most likely cause for the $\Delta\delta^{13}C$ increases in this period. This notion is

267   supported by the significant increases in the relative abundance of C_{21} and C_{25} *n*-alkanes

268   against the C_{31} *n*-alkane (Fig. 4c), because these homologues are predominantly found

269   in *Sphagnum* species (Ficken et al., 1998; Nott et al., 2000). Furthermore, the

270   magnitudes of the $\delta^{13}C$ offsets from the C_{31} *n*-alkane are ~ 3.4‰ for the C_{25} *n*-alkane

271   and ~ 3.8‰ for the C_{27} *n*-alkane, which match well with those observed in modern

272   *Sphagnum* species in which the $\delta^{13}C$ of the C_{25} and C_{27} *n*-alkanes are ~ 3.4‰ more

273   ^{13}C-depleted than the C_{31} *n*-alkane (Ficken et al., 1998). The potential contribution from

274   submerged/floating aquatic plants other than *Sphagnum* could have increased because

275   the C_{23} *n*-alkane is also abundant in these aquatic macrophytes (Ficken et al., 2000; Nott

276   et al., 2000). However, such vegetational changes are not supported by macrofossil

277   evidence from the Hani peat sequence (Schröder et al., 2007).

278   On the other hand, the pollen proxy record in nearby Lake Sihailongwan

279   revealed an increased influx from *Betula* between 14.3 to 14.0 ka (Stebich et al., 2009).

280   Because the C_{27} *n*-alkane is commonly found in *Betula* and *Fagus* trees (Table 1; Ali et

281   al., 2005; Sachse et al., 2006), parallel increases in the C_{27}/C_{31} and the $\Delta\delta^{13}C$ $(C_{31} - C_{27})$

282   from 14.4 to 14.1 ka (Fig. 4) might correspond to climate amelioration at the beginning

283   of the Late Glacial.

284   Relatively high P*aq* values and D-depleted hydrogen isotopic compositions of

285   the *n*-alkanes during 14 to 11 ka (Seki et al., 2009; Fig. 4) indicate that the increases in

286   aquatic plants likely are the consequence of enhanced water availability for the

287   peat-forming plants. In percolation mires like the Hani sequence, rainwater generally

288   flows over the peat surface and infiltrates the peat body during the wet growing season

289   due to the slope of the peat surface and the large amount of precipitation in the summer.

290   However, macrofossil records from the Hani mire suggest that the establishment of the

291   initial stage of percolation conditions did not occur until at least 12.6 ka (Schröder et al.,

292   2007). Hence, the water availability is likely to have been controlled by groundwater

293   level during this period although a marked rise in the total pollen concentrations and

294   increases in frequencies of moss and fern spores and the accumulation rate of biogenic

295   silica in nearby lake Sihailongwan suggest an increased precipitation during 14.5 to

296   13.6 ka (Stebich et al., 2007, 2009).

297

298   *3.2.2. Vegetational change from 12.7 to 11.6 ka*

299   Simultaneous increases in $\Delta\delta^{13}C$ ($C_{31} - C_{27}$) values and C_{27}/C_{31} ratios from

300   12.7 to 11.6 ka (Figs. 4b, d) indicate a relative increase of ^{13}C-depleted C_{27} *n*-alkanes

301   and/or a relative decrease of ^{13}C-depleted C_{31} *n*-alkanes during this time interval.

302   Because a certain *Sphagnum* species, *Sphagnum fuscum*, is known to have a large

303   abundance of the C_{27} *n*-alkane (Corrigan et al., 1973; Sachse et al., 2006; Yudina and

304   Savel'eva, 2008) and to contain C_{23}, C_{25} and C_{27} *n*-alkanes whose $\delta^{13}C$ are 1.3 to 2.0‰

305   lower than those of the C_{29} and C_{31} *n*-alkanes (Ficken et al., 1998; Xie et al., 2004), the

306   increased contribution of this species can consistently explain the high C_{27}/C_{31} ratios and

307   the increase in the $\Delta\delta^{13}C$ ($C_{31} - C_{23}$), $\Delta\delta^{13}C$ ($C_{31} - C_{25}$) and $\Delta\delta^{13}C$ ($C_{31} - C_{27}$) values

308   during the 12.7 to 11.6 ka period (Figs. 4a, b). The lack of change in the C_{23}/C_{31} ratios

309   suggests that the contribution of *Sphagnum* mosses did not increase, unlike the period

310   from 14.9 to 13.2 ka; however, it should be noted that the C_{23}/C_{31} ratio does not always

311   indicate an abundant *Sphagnum* contribution to peat deposits when the predominant

312   *Sphagnum* species possesses both the C_{27} and C_{31} *n*-alkanes as its major components

313   (Nott et al., 2000).

314   On the other hand, pollen records in nearby Lake Shihailongwan show

315   increases in the relative abundance of certain conifers (*Larix*, *Picea*) during the period

316   of Younger Dryas-like climate deterioration (12.4-11.7 ka; Stebich et al., 2007, 2009).

317   Because the leaf wax of these conifer trees contains the C_{31} *n*-alkane with a more

318   ^{13}C-enriched $\delta^{13}C$ value than the C_3 angiosperms (Chikaraishi and Naraoka, 2003;

319   Maffei et al., 2004; Pedentchouk et al., 2008), the high C_{27}/C_{31} and $\Delta\delta^{13}C$ values (Fig.

320   4) could be consequences of a relative decrease in the proportions of ^{13}C-depleted C_{31}

321   *n*-alkanes due to increases in conifer contributions.

322

323   **3.3. Climate changes in northeastern China recorded in the $\delta^{13}C$ of plant leaf**

324   **waxes**

325   Paleoclimate changes in northeast China for the last 16 ka are characterized

326   by a sequence of moisture changes. Various proxies document a general humidity

327   increase during the Late-glacial period with three short-term climate reversals to cool

328   and dry conditions at 13.9, 13.0 and 12.7 to 11.7 ka. In contrast, climate conditions in

329   the Holocene were relatively dry as compared to the deglacial period, however, the

330   summer monsoon rainfall record exhibits century-scale variability with maxima around

331   9.8 and 7.8 ka (An et al., 2000; Schettler et al., 2006; Stebich et al., 2007; Seki et al.,

332   2009; Zhou et al., 2010).

333   In Fig. 5, we compare the fluctuations of the $\delta^{13}C$ of terrestrial higher plant

334   *n*-alkanes (C_{29} and C_{31} *n*-alkanes) with those of the *n*-alkane averaged chain-length

335   (ACL) and the oxygen isotope compositions ($\delta^{18}O$) of Hani peat cellulose (Hong et al.,

336   2009a) in order to evaluate the influence of the paleoclimate changes on the $\delta^{13}C$

337   variations. The ACL value is the concentration-weighted mean chain-length of the C_{27},

338   C_{29} and C_{31} *n*-alkanes (Poynter et al., 1989), and its variations are commonly related to

339   changes in the temperature and aridity of the growing environment of alkane source

340   vegetation (Poynter et al., 1989; Kawamura et al., 2003; Schefuß et al., 2003;

341   Rommerskirchen et al., 2003). More recently, Sachse et al. (2006) reported a correlation

342   between the ACL and the hydrogen isotopic fractionation of leaf wax *n*-alkanes that

343   suggests that plants can alter the chain-lengths of their leaf waxes to minimize

344   evaporation of water vapor from their leaves. On the other hand, the cellulose $\delta^{18}O$ are

345   considered to reflect changes in surface air temperature (Hong et al., 2009a, b).

346   The ACL shows concomitant variations with the cellulose $\delta^{18}O$ (Fig. 5),

347   suggesting that the variations, in part, likely reflect plant physiological responses to

348   changes in temperature-driven evaporation. In contrast, the $\delta^{13}C$ of terrestrial higher

349   plant n-alkanes (C_{29} and C_{31} n-alkanes) exhibit fluctuations that are concurrent with the

350   ACL and $\delta^{18}O$ variations from 11.2 to 6.5 ka (light gray band in Fig. 5).

351   Stable carbon-isotopic fractionation (εp) of terrestrial higher plants is often

352   expressed as the following equation (Farquhar et al., 1982):

353    $$\varepsilon p = a + (b - a)\ C i/\ C a$$

354   where Ci/Ca is the ratio of CO_2 concentration in the intercellular space of leaves (Ci) to

355   that in the atmosphere (Ca); a is the fractionation associated with diffusion of CO_2 from

356   the atmosphere into the intercellular space of leaves (4.4‰) and b is the fractionation of

357   CO_2 during carboxylation mediated by Rubisco (ca. 30‰). With higher evaporation

358   rates, plants would have reduced stomatal conductance to minimize the evaporative loss

359   of water from their leaves and thereby lowering Ci/Ca, which results in the $\delta^{13}C$ of the

360   plants becoming more ^{13}C enriched, and vice versa. Hence, the concurrent fluctuations

361   between the $\delta^{13}C$ and the ACL values during the early Holocene indicate that the $\delta^{13}C$

362   variations reflect plant physiological responses to changes in net evaporation in Hani

363   region during the early Holocene.

364   Nevertheless, it should be noted that the $\delta^{13}C$ variations of terrestrial higher

365   plant n-alkanes (C_{29} and C_{31} n-alkanes) do not match with the ACL variations in the 15.5

366   to 11.4 ka and 6.5 to 0.1 ka intervals (Fig. 5). This absence of agreement could be partly

367   related to the origin of the n-alkanes, because the C_{29} and C_{31} n-alkanes can also be

368   produced by several mosses found in the Hani peatland (Table 1) besides terrestrial

369   higher plant leaf waxes. Isotopic fractionation during carbon fixation in mosses is

370   generally smaller than in other peat-forming plants due to the lack of functional stomata

371   and a waxy cuticle on the leaf epidermis (Xie et al., 2004), and thus potential increases

372   in n-alkane inputs from mosses during wetter periods in the Late Glacial and in late

14

373   Holocene may conceal the $\delta^{13}C$ signals recorded in the *n*-alkanes derived from

374   evaporation-sensitive terrestrial higher plant.

375   Several lines of evidence indicate short-term enhancement of summer

376   monsoon rainfall in eastern China during the early Holocene. Wang et al. (1999)

377   examined the $\delta^{18}O$ of planktonic foraminifera in South China Sea sediments and

378   concluded that monsoon runoff and precipitation increased at ca. 9.4 and 8–8.1 ka in

379   southeast China. Nearly simultaneously, the net accumulation rate of biogenic silica

380   decreased (Schettler et al., 2006) and the $\delta^{13}C$ values of peat cellulose (Hong et al.,

381   2005) increased at 9.5 and 8.0 ka in northeast China (Fig. 5d), indicating an enhanced

382   summer monsoon rainfall at that time. Our *n*-alkane $\delta^{13}C$ records of terrestrial higher

383   plant *n*-alkanes (C_{29} and C_{31} *n*-alkanes) exhibit 1.4 to 1.8‰ negative shifts with the ACL

384   increases at 10.5–9.3 ka and 8.1 ka (dark gray bands in Fig. 5), which is likely to

385   represent the $\delta^{13}C$ responses of peat-forming terrestrial higher plant to the increases in

386   summer monsoonal precipitation in eastern China.

387   In northeast China, seasonal and inter-annual changes in temperature and

388   precipitation are connected with activity of the summer and winter monsoon. Most of

389   the annual precipitation is derived from the summer monsoon, and the distribution of

390   annual precipitation shows a gradual decrease toward the north-west. These

391   spatiotemporal patterns in monsoonal precipitation indicate that the short-term onset

392   and fluctuations of the summer monsoon strength may have significantly influenced the

393   early Holocene variations in effective precipitation in the Hani region.

394

395   **4. Summary and conclusions**

396   Compound-specific $\delta^{13}C$ values of C_{21} to C_{33} odd carbon number *n*-alkanes

397   (–36.6 to –30.7‰) were measured in the Hani peat deposit from northeast China to

398   assess possible changes in source vegetation and to reconstruct the regional

399   paleoclimatic history over the last 16 ka. Major changes were found in the isotopic and

400 molecular compositions of *n*-alkanes and are interpreted as follows.

401 　　　1. The $\delta^{13}C$ profiles of individual *n*-alkanes show decoupled fluctuation

402 patterns particularly in the 960 to 650 cm interval (15.5 to 11.4 ka). A comparison

403 between the $\delta^{13}C$ offsets among individual *n*-alkane records ($\Delta\delta^{13}C$) and biomarker

404 paleoplant proxies (P*aq*, C_{23}/C_{31}, and C_{27}/C_{31}) reveal concurrent increases in C_{23}/C_{31}

405 ratios and $\Delta\delta^{13}C$ values from 14.9 to 13.2 ka that were most likely a result of enhanced

406 flourishing of *Sphagnum* plants (moss) during this time interval.

407 　　　2. Larger C_{27}/C_{31} ratios and increases in $\Delta\delta^{13}C$ ($C_{31} - C_{27}$) and $\Delta\delta^{13}C$ ($C_{31} -$

408 C_{25}) occur in peat deposited from 12.7–11.6 ka. These changes are likely a consequence

409 of an increased relative contribution of ^{13}C-depleted C_{27}-dominated *Sphagnum* species

410 and/or a decreased contribution of ^{13}C-depleted C_{31} *n*-alkane due to the expansion of

411 conifers.

412 　　　3. Parallel fluctuations between the $\delta^{13}C$ values of terrestrial higher

413 plant-derived *n*-alkanes (C_{29} and C_{31}) and the *n*-alkane average chain-length (ACL)

414 values during the early Holocene suggest that the $\delta^{13}C$ variation most likely reflect plant

415 physiological responses to changes in effective precipitation (i.e., precipitation minus

416 evaporation).

417 　　　4. The $\delta^{13}C$ variations exhibit 1.4 to 1.8‰ negative shifts at 10.5–9.3 ka and

418 8.1 ka along with decreased ACL values, indicating that the effective precipitation in

419 northeastern China was variable during the early Holocene, probably due to short-term

420 enhancement of summer monsoon rainfall at that time.

421

16

429

429 **References**

430 Ali, H. A. M., Mayes, R. W., Hector, B. L., Verma, A. K., Ørskov, E. R., 2005. The

431   possible use of n-alkanes, long-chain fatty alcohols and long-chain fatty acids

432   as markers in studies of the botanical composition of the diet of free-ranging

433   herbivores. Journal of Agricultural Science 143, 85–95.

434 Arens, N. C., Jahren, A. H., Amundson, R., 2000. Can C3 plants faithfully record the

435   carbon isotopic composition of atmospheric carbon dioxide? Paleobiology 26,

436   137–164.

437 An, Z., Porter, S. C., Kutzbach, J. E., Wu, X., Wang, S., Liu, X., Li, Z., Zhou, W., 2000.

438   Asynchronous Holocene optimum of the East Asian monsoon. Quaternary

439   Science Reviews 19, 743–762.

440 Baas, M., Pancost, R., van Geel, B., Sinninghe Damsté, J. S., 2000. A comparative study

441   of lipids in *Sphagnum* species. Organic Geochemistry 31, 535–541.

442 Baker, A., Caseldine, C. J., Gilmour, M. A., Charman, D., Proctor, C. J., Hawkesworth,

443   C. J., Pillips, N., 1999. Stalagmite luminescence and peat humification records

444   of palaeomoisture for the last 2500 years. Earth and Planetary Science Letters

445   165, 157–162.

446 Barber, K. E., 1985. Peat stratigraphy and climatic change: Some speculations. In:

447   Tooley, M. J., Sheail, G. M. (Eds.), The Climatic Scene: Essays in Honour of

448   Gordon Manley. Allen and Unwin, London. pp. 175–185.

449 Bendle, J., Kawamura, K., Yamazaki, K., Niwai, T., 2007. Latitudinal distribution of

450   terrestrial lipid biomarkers and *n*-alkane compound-specific stable carbon

451   isotope ratios in the atmosphere over the western Pacific and Southern Ocean.

452   Geochimica et Cosmochimica Acta 71, 5934–5955.

453 Blackford, J. J., 2000. Paleoclimate records from peat. Trends in Ecology & Evolution

454   15, 193–195.

455 Blackford, J. J., Chambers, F. M., 1993. Determining the degree of peat decomposition

456   in peat-based palaeoclimatic studies. International Peat Journal 5, 7–24.

457   Charman, D. J., 2001. Biostratigraphic and Palaeoenvironmental applications of testate

458   amoebae. Quaternary Science Reviews 20, 1753–1764.

459   Chikaraishi, Y., Naraoka, H., 2003. Compound-specific δD-$\delta^{13}C$ analyses of n-alkanes

460   extracted from terrestrial and aquatic plants. Phytochemistry 63, 361–371.

461   Collister, J. W., Rieley, G., Stern, B., Eglington, G., Fry, B., 1994. Compound-specific

462           $\delta^{13}C$ analyses of leaf lipids from plants with differing carbon dioxide

463   metabolisms. Organic Geochemistry 21, 619–627.

464   Corrigan, D., Kloos, C., O'Connor, C. S., Timoney, R. F., 1973. Alkanes from four

465   species of *Sphagnum* moss. Phytochemistry 12, 213–214.

466   Cranwell, P. A., 1984. Lipid geochemistry of sediments from Upton Broad, a small

467   productive lake. Organic Geochemistry. 7, 25–37.

468   Eglinton, G., Hamilton, R. J., 1967. Leaf epicuticular waxes. Science 156, 1322–1335.

469   Farquhar, G. D., O'leary, M. H., Berry, J. A., 1982. On the relationship between carbon

470   isotope discrimination and the intercellular carbon dioxide concentration in

471   leaves. Australian Journal of Plant Physiology 9, 121–137.

472   Ficken, K. J., Barber, K. E., Eglinton, G., 1998. Lipid biomarker, $\delta^{13}C$ and plant

473   macrofossil stratigraphy of a Scottish montane peat bog over the last two

474   millennia. Organic Geochemistry 28, 217–237.

475   Ficken, K. J., Li, B., Swain, D. L., Eglinton, G., 2000. An *n*-alkane proxy for the

476   sedimentary input of submerged/floating freshwater aquatic macrophytes.

477   Organic Geochemistry 31, 745–749.

478   Hong, Y. T., Wang, Z. G., Jiang, H. B., Lin, Q. H., Hong, B., Zhu, Y. X., Wang, Y., Xu,

479   L. S., Leng, X. T., Li, H. D., 2001. A 6000-year record of changes in drought

480   and precipitation in northeastern China based on a $\delta^{13}C$ time series from peat

481   cellulose. Earth and Planetary Science Letters 185, 111–119.

482   Hong, Y. T., Hong, B., Lin, Q. H., Shibata, Y., Hirota, M., Zhu, Y. X., Leng, X. T., Wang,

483   Y., Wang, H., Yi, L., 2005. Inverse phase oscillations between the East Asian

484   and Indian Ocean summer monsoons during the last 12000 years and paleo-El

485   Niño. Earth and Planetary Science Letters 231, 337–346.

486   Hong, B., Liu, C. Q., Lin, Q. H., Shibata, Y., Leng, X. T., Wang, Y., Zhu, Y. X., Hong, Y.

487   T., 2009a. Temperature evolution from the $\delta^{18}O$ record of Hani peat, Northeast

488   China, in the last 14000 years. Science in China Series D: Earth Sciences 52,

489   952–964.

490   Hong, Y. T., Hong, B., Lin, Q. H., Shibata, Y., Zhu, Y. X., Leng, X. T., Wang, Y., 2009b.

491   Synchronous climate anomalies in the western North Pacific and North

492   Atlantic regions during the last 14,000 years. Quaternary Science Reviews 28,

493   840–849.

494   Kawamura, K., Ishimura, Y., Yamazaki, K., 2003. Four years' observations of terrestrial

495   lipid class compounds in marine aerosols from the western North Pacific.

496   Global Biogeochemical Cycles 17, 1003.

497   Leuenberger, M., Siegenthaler, U., Langway, C. C., 1992. Carbon isotope composition

498   of atmospheric CO_2 during the last ice age from an Antarctic ice core. Nature

499   357, 488–490.

500   López-Díaz, V., Borrego, Á.G., Blanco, C.G., Aboleya, M., López-Sáez, J.A.,

501   López-Merino, L., 2010. Biomarkers in a peat deposit in Northern Spain

502   (Huelga de Bayas, Asturias) as a proxy for climate variation. Journal of

503   Chromatography A 1217, 3538–3546.

504   Maffei, M., Badino, S., Bossi, S., 2004. Chemotaxonomic significance of leaf wax

505   n-alkanes in the Pinales (Coniferales). Journal of Biological Research 1, 3–19.

506   Meyers, P. A., 2003. Applications of organic geochemistry to paleolimnological

507   reconstructions: a summary of examples from the Laurentian Great Lakes.

508   Organic Geochemistry 34, 261–289.

509   Makohonienko, M., Kitagawa, H., Fujiki, T., Liu, X., Yasuda, Y., Yin, H., 2008. Late

510   Holocene vegetation changes and human impact in the Changbai Mountains

511   area, Northeast China. Quaternary International 184, 94–108.

512 Nichols, J., Booth, R. K., Jackson, S. T., Pendall, E. G., Huang, Y., 2006.

513   Paleohydrologic reconstruction based on *n*-alkane distributions in

514   ombrotrophic peat. Organic Geochemistry 37, 1505–1513.

515 Nott, C. J., Xie, S., Avsejs, L. A., Maddy, D., Chambers, F. M., Evershed, R. P., 2000.

516   *n*-Alkane distributions in ombrotrophic mires as indicators of vegetation

517   change related to climatic variation. Organic Geochemistry 31, 231–235.

518 Pancost, R. D., Baas, M., van Geel, B., Sinninghe Damsté, J. S., 2002. Biomarkers as

519   proxies for plant inputs to peats: an example from a sub-boreal ombrotrophic

520   bog. Organic Geochemistry 33, 675–690.

521 Pedentchouk, N., Sumner, W., Tipple, B., Pagani, M., 2008. δ^{13}C and δD compositions

522   of *n*-alkanes from modern angiosperms and conifers: An experimental set up

523   in central Washington State, USA. Organic Geochemistry 39, 1066–1071.

524 Pendall, E., Markgraf, V., White, J.W.C., Dreier, M., Kenny, R., 2001. Multiproxy

525   record of Late Pleistocene-Holocene climate and vegetation changes from a

526   peat bog in Patagonia. Quaternary Research 55, 168–178.

527 Poynter, J. G., Farrimond, P., Robinson, N., Eglinton, G., 1989. Aeolian-derived higher

528   plant lipids in the marine sedimentary record: links with palaeoclimate. In:

529   Leinen, M., Sarnthein, M. (Eds.) Paleoclimatology and paleometeorology:

530   modern and past patterns of global atmospheric transport. Kluwer Academic

531   Publishers, Dordrecht, The Netherlands. pp. 435–462.

532 Rao, Z., Zhu, Z., Jia, G., Henderson, A. C. G., Xue, Q., Wang, S., 2009. Compound

533   specific δD values of long chain *n*-alkanes derived from terrestrial higher

534   plants are indicative of the δD of meteoric waters: Evidence from surface soils

535   in eastern China. Organic Geochemistry 40, 922–930.

536 Rieley, G., Collier, R. J., Jones, D. M., Eglinton, G., Eakin, P. A., Fallick, A. E., 1991.

537   Sources of sedimentary lipids deduced from stable carbon-isotope analyses of

538   individual compounds. Nature 352, 425–427.

539   Rommerskirchen, F., Eglington, G., Dupont, L., Günter, U., Wenzel, C., Rullkötter, J.,

540   2003. A north to south transect of Holocene southeast Atlantic continental

541   margin sediments: Relationship between aerosol transport and

542   compound-specific δ^{13}C land plant biomarker and pollen records.

543   Geochemistry, Geophysics, Geosystems 4(12), 1101.

544   Sachse, D., Radke, J., Gleixner, G., 2006. δD values of individual *n*-alkanes from

545   terrestrial plants along a climatic gradient – Implications for the sedimentary

546   biomarker record. Organic Geochemistry 37, 469–483.

547   Schefuβ, E., Ratmeyer, V., Stuut, J.-B. W., Jansen, J. H. F., Sinninghe Damsté, J. S.,

548   2003. Carbon isotope analysis of *n*-alkanes in dust from the lower atmosphere

549   over the central eastern Atlantic. Geochimica et Cosmochimica Acta 67,

550   1757–1767.

551   Schettler, G., Liu, Q., Mingram, J., Stebich, M., Dulski, P., 2006. East-Asian monsoon

552   variability between 15000 and 2000 cal. yr BP recorded in varved sediments of

553   Lake Sihailongwan (northeastern China, Long Gang volcanic field). The

554   Holocene 16, 1043–1057.

555   Schröder, C., Thiele, A., Wang, S, Bu, Z., Joosten, H., 2007. Hani-mire – A percolation

556   mire in northeast China. Peatlands International 2, 21–24.

557   Schwark, L., Zink, K., Lechterbeck, J., 2002. Reconstruction of postglacial to early

558   Holocene vegetation history in terrestrial Central Europe via cuticular lipid

559   biomarkers and pollen records from lake sediments. Geology 30, 463–466.

560   Seki, O., Meyers, P. A., Kawamura, K., Zheng, Y., Zhou, W., 2009. Hydrogen isotopic

561   ratios of plant-wax *n*-alkanes in a peat bog deposited in northeast china during

562   the last 16kyr. Organic Geochemistry 40, 671–677.

563   Stebich, M., Arlt, J., Mingram, J., 2007. Late Quaternary vegetation history of N. E.

564   China – recent progress in the investigation of Sihailongwang maar lake. In:

565   Kahlke, R.-D. Maul, L. C., Mazza, P. (Eds.), Late Neogene and Quaternary

566   biodiversity and evolution: regional developments and interregional

567   correlations (Proceedings of the 18th international Senckenberg Conference

568   (VI International Palaeontological Colloquium in Weimar)). Courier

569   Forschungsinstitut Senckenberg 259, Stuttgart. pp. 181–190.

570 Stebich, M., Mingram, J., Han, J., Liu, J., 2009. Late Pleistocene spread of

571   (cool-)temperate forests in Northeast China and climate changes synchronous

572   with the North Atlantic region. Global and Planetary Change 65, 56–70.

573 Stuiver, M., Reimeer, P.J., 1993. Extended ^{14}C database and revised Calib 3.1 ^{14}C age

574   calibration program. Radiocarbon 35, 215–230.

575 Stuiver, M., Reimer, P.J., Bard, E., Beck, J.W., Burr, G.S., Hughen, K.A., Kromer, B.,

576   McCormac, G., Van der Plicht, J., Spurk, M., 1998. INTCAL98 Radiocarbon

577   age calibration. Radiocarbon 40, 1041–1083.

578 Yamamoto, S., Kawamura, K., 2010. Application of urea adduction technique to

579   polluted urban aerosols for the determination of hydrogen isotopic

580   composition of *n*-alkanes. International Journal of Environmental Analytical

581   Chemistry, in press.

582 Yudina, N. V., Savel'eva, A. V., 2008. Hydrocarbons in peat-forming plants at eutrophic

583   bogs in western Siberia. Geochemistry International 46, 77–84.

584 Wang, H., Hong, Y., Zhu, Y., Hong, B., Lin, Q., Xu, H., Leng, X., Mao, X., 2004.

585   Humification degrees of peat in Qinghai-Xizang Plateau and palaeoclimate

586   change. Chinese Science Bulletin 49, 514–519.

587 Wang, L., Sarnthein, M., Erlenkeuser, H., Grootes, P. M., Grimalt, J. O., Pelejero, C.,

588   Linck, G., 1999. Holocene variations in Asian monsoon moisture: a bidecadal

589   sediment record from the South China Sea. Geophysical Research Letters 26,

590   2889–2892.

591   Xie, S., Nott, C. J., Avsejs, L. A., Maddy, D., Chambers, F. M., Evershed, R. P., 2004.

592   Molecular and isotopic stratigraphy in an ombrotrophic mire for paleoclimate

593   reconstruction. Geochimica et Cosmochimica Acta 68, 2849–2862.

594   Xu , H., Hong, Y., Lin, Q., Zhu, Y., Hong, B., Jiang, H., 2006. Temperature responses to

595   quasi-100-yr solar variability during the past 6000 years based on $\delta^{18}O$ of peat

596   cellulose in Hongyuan, eastern Qinghai–Tibet plateau, China.

597   Palaeogeography, Palaeoclimatology, Palaeoecology 230, 155–164.

598   Zheng, Y., Zhou, W., Meyers, P. A., Xie, S., 2007. Lipid biomarkers in the

599   Zoigê-Hongyuan peat deposit: Indicators of Holocene climate changes in West

600   China. Organic Geochemistry 38, 1927–1940.

601   Zhou, W., Xie, S., Meyers, P. A., Zheng, Y., 2005. Reconstruction of late glacial and

602   Holocene climate evolution in southern China from geolipids and pollen in the

603   Dingnan peat sequence. Organic Geochemistry 36, 1272–1284.

604   Zhou, W., Zheng, Y., Meyers, P. A., Jull, A. J. T., Xie, S., 2010. Postglacial

605   climate-change record in biomarker lipid compositions of the Hani peat

606   sequence, northeastern China. Earth and Planetary Science Letters 294, 37–46.

607

Table 1
Summary of dominant *n*-alkane homologues in modern plant taxa found at Hani peatland

Plant species (Hong et al., 2005)		Dominant *n*-alkane homologues	References
Sphagnum	*palustre*	C23>C25	Nott et al. (2000), Baas et al. (2000)
S.	*magellamicum*	C31>C25>C29, C25	Nott et al. (2000), Baas et al. (2000)
S.	*acutifolium*		
Polytrichum	*commune*	C31>C29>C33[a]	Nott et al. (2000)
Calliergonella	*cuspidata*		
Eriphorum	*vaginatum*	C31>C33>C29	Nott et al. (2000)
Carex	*schmidtii*		
C.	*tenuiflora*	C31>C33>C29[a]	Nichols et al. (2006)
Phragmitex	*communis*		
Typha	*latifolia*	C29>C27	Cranwell (1984)
Equisetum	*heleocharis*		
Comarum	*palustre*		
Larix	*olgensis*	C31[a]	Maffei et al. (2004)
Betula	*ovalifolia*	C27, C31[a]	Sachse et al. (2006)
Vaccinium	*uliginosum*	C29>C31>C27[a]	Nott et al. (2000)
Ledum	*palustre var. dilatatum*		
L.	*palustre var. angustum*		
Chamaedaphne	*calyculata*	C29>C31	Nichols et al. (2006)

[a] Data adapted from different or unspecified species within the same genera.

607

608

609

Figure captions

610

611 **Fig. 1.** Map showing the location of the Hani peat bog, northeast China.

612

613 **Fig. 2.** Stratigraphic section of the Hani peat sequence with chronology and histograms

614 of distributions of *n*-alkanes. Note that *n*-alkane distribution in the lower part of the

615 column exhibits important contributions of mid-chain components from mosses. Cal

616 ages are obtained from accelerator mass spectrometry (AMS) ^{14}C ages that were

617 provided by Zhou et al. (2010).

618

619 **Fig. 3.** Depth profiles of carbon isotope ratios (δ^{13}C) of C_{21} to C_{33} odd carbon number

620 *n*-alkanes.

621

622 **Fig. 4.** Profiles of (a), (b) the δ^{13}C offsets ($\Delta\delta^{13}$C) between the C_{31} *n*-alkane and the C_{21},

623 C_{23}, C_{25}, C_{27}, C_{29} and C_{33} *n*-alkanes, (c), (d) the concentration ratios of the C_{21} to C_{29} odd

624 carbon number *n*-alkanes and the C_{33} *n*-alkane against the C_{31} *n*-alkane, and (e), (f) the

625 P*aq* and the δD of the C_{27} *n*-alkane (Seki et al., 2009) over the last 16 ka. Shaded bands

626 indicate the intervals where the $\Delta\delta^{13}$C offsets show concomitant variations with the
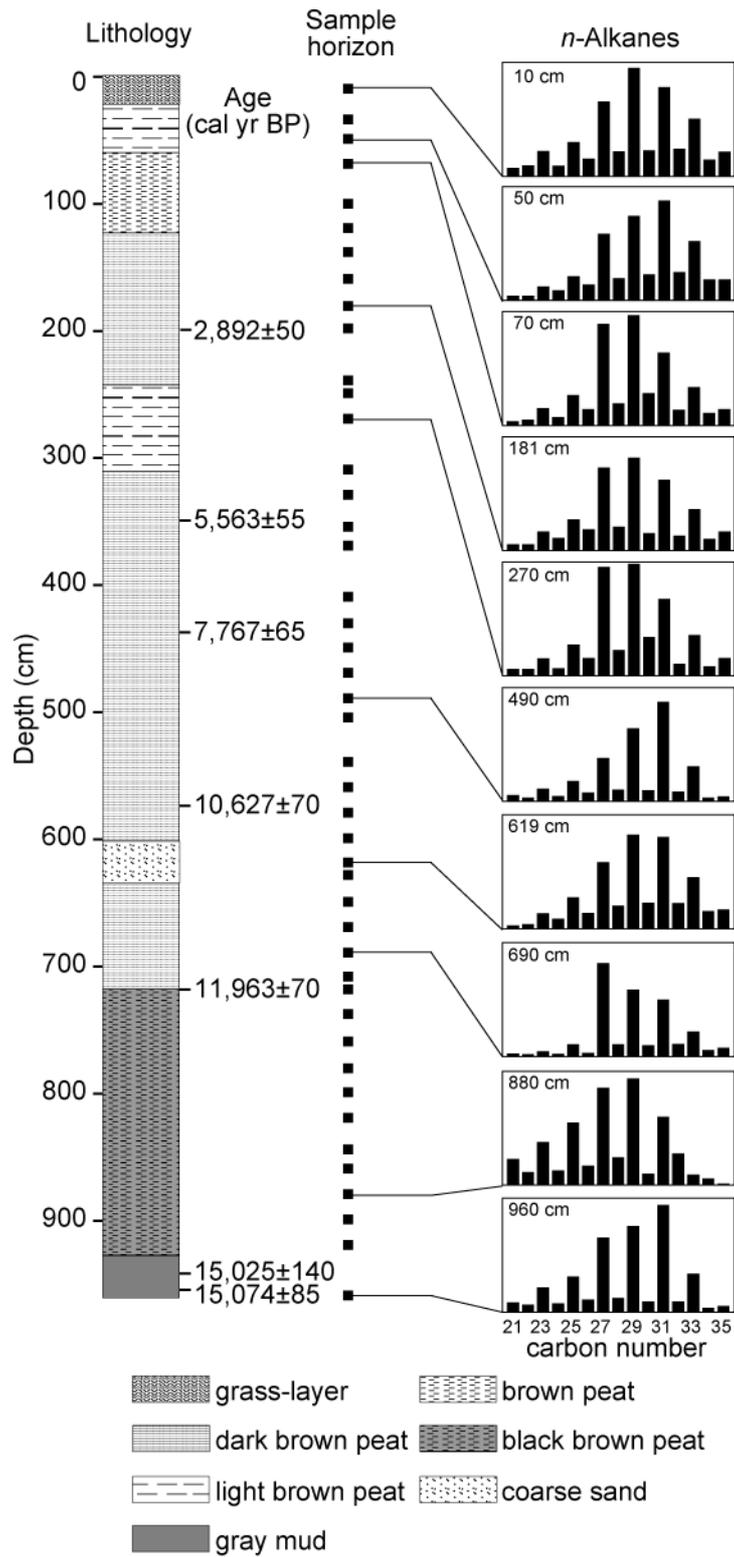
627 *n*-alkane ratios.

628

629 **Fig. 5.** Variations of (a) the δ^{13}C of terrestrial higher plant-derived *n*-alkanes (C_{29} and

630 C_{31} *n*-alkanes), (b) the ACL, and (c) the δ^{18}O (Hong et al., 2009a) and (d) δ^{13}C of peat

631 cellulose (Hong et al., 2005) in the Hani peat bog. The δ^{13}C of C_{29} and C_{31} *n*-alkanes and

632 the ACL show parallel fluctuations in a light gray shaded sequence with minimal values

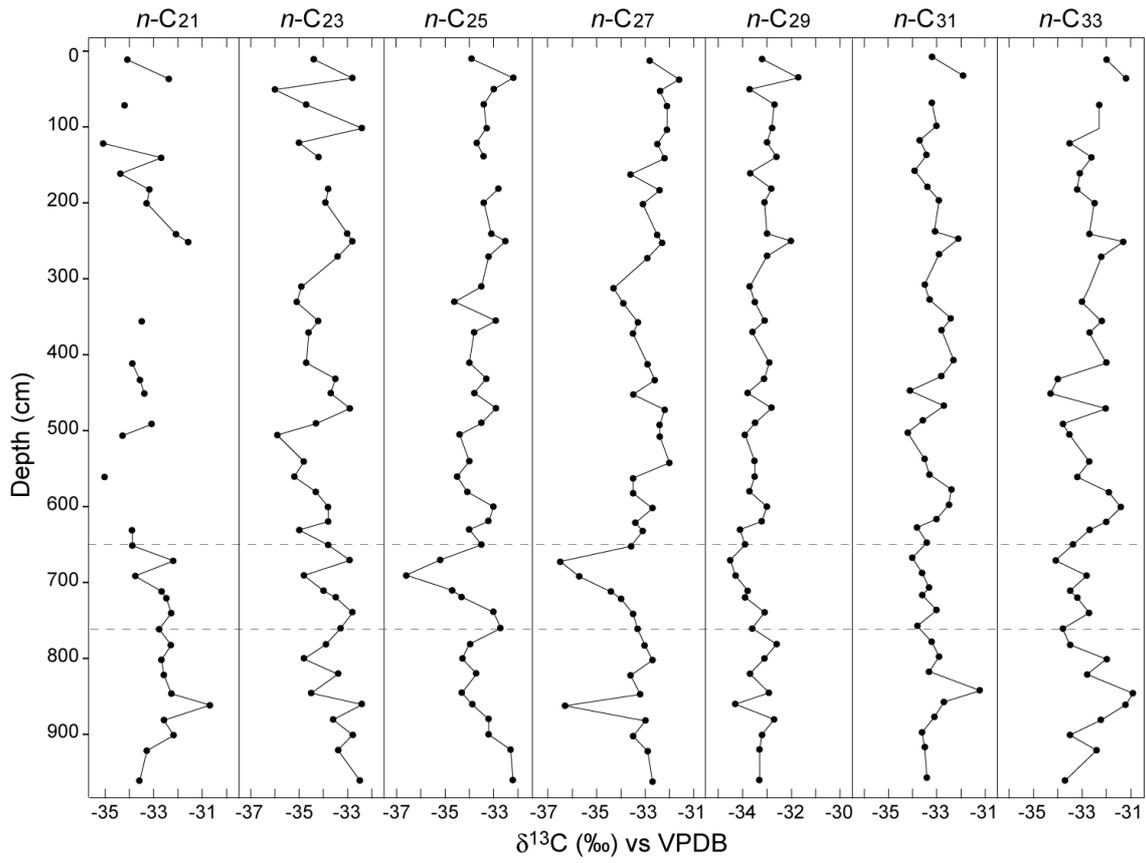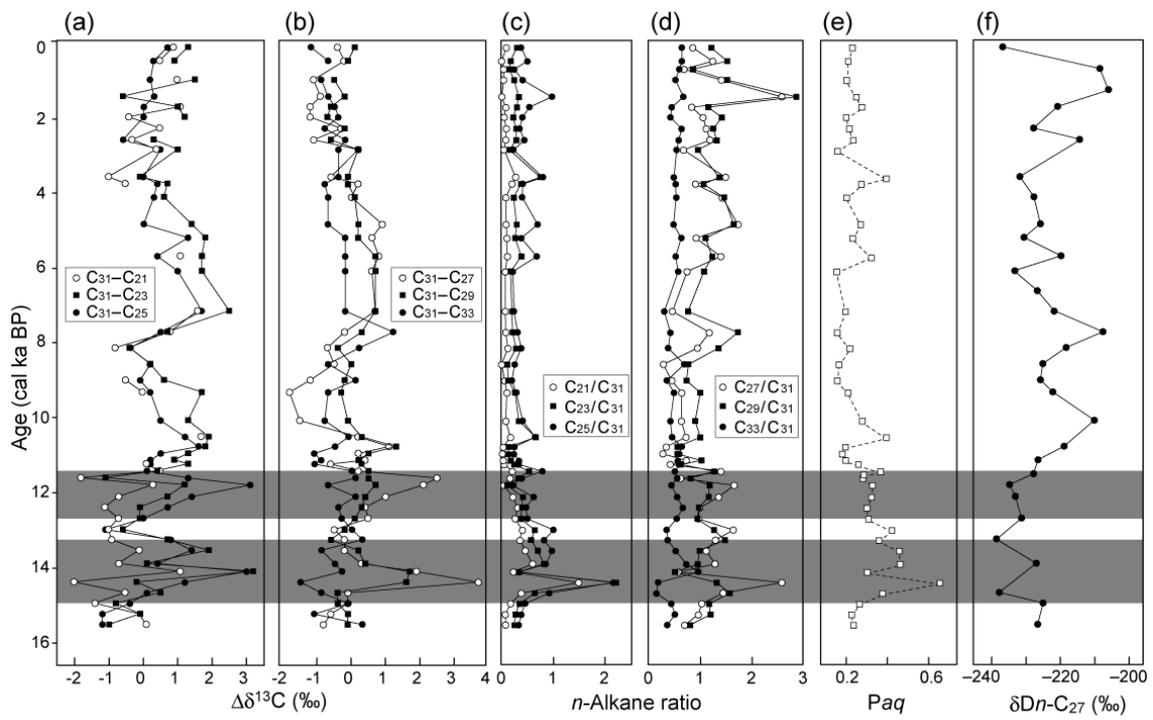633 at 10.5–9.3 ka and 8.1 ka (dark gray bands).

634

634

635

636 Fig. 1

637

Fig. 2

Fig. 3

643

644

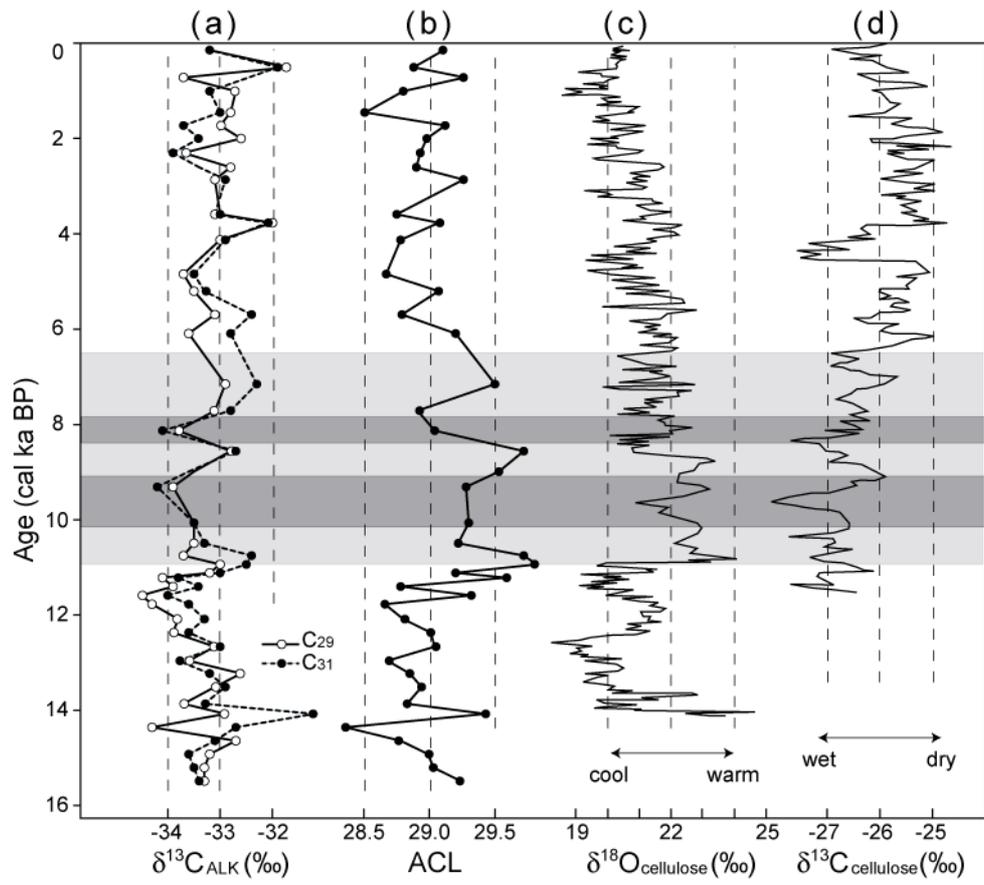645   Fig. 4

646

646

647

648   Fig. 5